DOI: 10.1534/genetics.107.070813

Clustering of Genetically Defined Allele Classes in the *Caenorhabditis elegans* DAF-2 Insulin/IGF-1 Receptor

Dhaval S. Patel,*[,1] Acely Garza-Garcia,[†,‡] Manoj Nanji,* Joshua J. McElwee,*[,2] Daniel Ackerman,* Paul C. Driscoll[†,‡] and David Gems*[,3]

**Department of Biology, and [†]Department of Biochemistry and Molecular Biology, University College London, London WC1E 6BT, United Kingdom and [‡]Division of Molecular Structure, National Institute for Medical Research, London NW7 1AA, United Kingdom*

Manuscript received January 11, 2007
Accepted for publication November 27, 2007

ABSTRACT

The DAF-2 insulin/IGF-1 receptor regulates development, metabolism, and aging in the nematode *Caenorhabditis elegans*. However, complex differences among *daf-2* alleles complicate analysis of this gene. We have employed epistasis analysis, transcript profile analysis, mutant sequence analysis, and homology modeling of mutant receptors to understand this complexity. We define an allelic series of nonconditional *daf-2* mutants, including nonsense and deletion alleles, and a putative null allele, *m65*. The most severe *daf-2* alleles show incomplete suppression by *daf-18(0)* and *daf-16(0)* and have a range of effects on early development. Among weaker *daf-2* alleles there exist distinct mutant classes that differ in epistatic interactions with mutations in other genes. Mutant sequence analysis (including 11 newly sequenced alleles) reveals that class 1 mutant lesions lie only in certain extracellular regions of the receptor, while class 2 (pleiotropic) and nonconditional missense mutants have lesions only in the ligand-binding pocket of the receptor ectodomain or the tyrosine kinase domain. Effects of equivalent mutations on the human insulin receptor suggest an altered balance of intracellular signaling in class 2 alleles. These studies consolidate and extend our understanding of the complex genetics of *daf-2* and its underlying molecular biology.

IN mammals, insulin and insulin-like growth factor 1 (IGF-1) receptors are major regulators of energy homeostasis and growth, respectively. In invertebrates such as the nematode *Caenorhabditis elegans* and the fruit fly *Drosophila melanogaster*, a single insulin/IGF-1 signaling pathway acts as a major regulator of life history. For example, reduction of insulin/IGF-1 signaling can increase life span in both organisms (Friedman and Johnson 1988; Kenyon *et al.* 1993; Clancy *et al.* 2001; Tatar *et al.* 2001; Ayyadevara *et al.* 2007). Insulin/IGF-1 signaling may also function as a regulator of aging in mammals, since global reduction of IGF-1 receptor function or of fat-specific reduction of insulin receptor function can increase life span in mice (Bluher *et al.* 2003; Holzenberger *et al.* 2003).

In *C. elegans*, the insulin/IGF-1 receptor is encoded by the gene *daf-2* (Kimura *et al.* 1997). An intracellular pathway similar to the cognate mammalian and Drosophila pathways acts downstream of the DAF-2 receptor. This includes an AAP-1/AGE-1 phosphatidylinositol 3-kinase (PI 3-kinase) (Morris *et al.* 1996; Wolkow *et al.* 2002) and PDK-1, AKT-1, AKT-2, and SGK-1 serine/threonine kinases (Paradis and Ruvkun 1998; Paradis *et al.* 1999; Hertweck *et al.* 2004).

Mutations reducing activity of many genes in this pathway can cause constitutive formation of dauer larvae (the Daf-c phenotype). The dauer larva is a facultative diapausal form of third-stage larva, which forms in response to several environmental cues linked with conditions that are not propitious for reproduction (Cassada and Russell 1975; Riddle and Albert 1997).

AKT-1, AKT-2, and SGK-1 phosphorylate and inactivate the FOXO transcription factor DAF-16 (Lin *et al.* 1997; Ogg *et al.* 1997), whose activity is necessary for the dauer constitutive (Daf-c) and longevity (Age) traits resulting from reduced insulin/IGF-1 signaling (Kenyon *et al.* 1993; Riddle and Albert 1997). Phosphorylation inactivates DAF-16 at least in part by causing its sequestration in the cytoplasm (Henderson and Johnson 2001; Lee *et al.* 2001; Lin *et al.* 2001).

Analysis of genetic epistasis has been an important tool in helping to establish the order in which genes function in pathways in *C. elegans* (Avery and Wasserman 1992; Huang and Sternberg 1995). In studies of *daf-2*, epistasis analysis has been complicated by the fact that different *daf-2* alleles can behave very differently. For example, mutational loss of function of *daf-12*, which

[1]*Present address:* Department of Biological Structure, School of Medicine, University of Washington, Seattle, WA 98195-7270.

[2]*Present address:* Rosetta Inpharmatics, Seattle, WA 98109.

[3]*Corresponding author:* Department of Biology, University College London, Gower St., London WC1E 6BT, United Kingdom.
E-mail: david.gems@ucl.ac.uk

encodes a nuclear hormone receptor (Antebi *et al.* 2000), suppresses the Daf-c phenotype of *daf-2(m41)*. Yet when added to *daf-2(e1370)*, *daf-12* can result in early larval arrest (Vowels and Thomas 1992; Larsen *et al.* 1995), even though in terms of Daf-c, *e1370* is a weaker allele than *m41* (Gems *et al.* 1998). Moreover, while *daf-12 (m20)* partially suppresses the longevity increase of *daf-2(m41)*, it enhances that of *daf-2(e1370)* (Larsen *et al.* 1995).

Such allele-specific effects reflect the presence of distinct phenotypic classes of the *daf-2* mutant (Gems *et al.* 1998). Most *daf-2* reduction-of-function (hypomorphic) alleles form a single, approximate allelic series over a range of severity. Weak alleles cause weak temperature-sensitive (ts) Daf-c and Age phenotypes; severe alleles cause strong ts Daf-c and non-ts Age phenotypes, plus other ts pleiotropic traits, such as reduced feeding (Eat) and reduced movement (Unc). However, some *daf-2* alleles do not fit within this scheme, exhibiting relatively severe ts Daf-c phenotypes, but not the additional pleiotropic traits. In such alleles, *e.g.*, *e1369, m41* and *m212*, Daf-c is also suppressed by *daf-12(m20)*. On this basis, *daf-2* alleles were classified into class 1 (Daf-c, Age: suppressed by *daf-12*), and class 2 (Daf-c, Age, plus other pleiotropic traits: enhanced by *daf-12*) (Gems *et al.* 1998).

daf-2 allele-specific effects of the type seen with interactions with *daf-12* are also seen with other components of the *daf-12* pathway. These include the *daf-9* sterol monooxygenase (Gerisch *et al.* 2001; Motola *et al.* 2006), the *daf-12* cofactor *din-1S* (Ludewig *et al.* 2004), and the dafachronic acid steroid ligands for *daf-12* (Motola *et al.* 2006). Examples of *daf-2* allelic differences are summarized in Table 1.

In this study we have investigated the molecular changes that underlie phenotypic differences among *daf-2* alleles. We have extended the description of the phenotypes of *daf-2* with respect to nonconditional mutants and characterized the molecular lesions in 11 *daf-2* mutants, including many unusual alleles. We have also examined the predicted effects of mutations on the DAF-2 receptor using three-dimensional homology modeling (Garza-Garcia *et al.* 2007) and other approaches. Taken together, our findings provide a clearer and more detailed overview of the genetics of *daf-2*.

MATERIALS AND METHODS

Nematode culture and strains: Procedures for growth and manipulation of *C. elegans* were as published (Brenner 1974; Sulston and Hodgkin 1988). *C. elegans* strains employed included the following: wild type—N2 Bristol (CGC male stock) (Gems and Riddle 2000), CF1844 *fer-15(b26); daf-2(mu150); fem-1(hc17)*, DR608 *daf-2(m212)*, DR1436 *daf-2(m631)/qC1* [*dpy-19(e1259ts) glp-1(q339)*], DR1468 *daf-2(m646)/qC1*, DR1563 *daf-2(e1370)*, DR1564 *daf-2(m41)*, DR1566 *daf-2(m579)*, DR1567 *daf-2(m577)*, DR1568 *daf-2(e1371)*, DR1573 *daf-2(e1369)*, DR1942 *daf-2(e979)*, GA302 *daf-2(tm1236)/qC1*, GR1307 *daf-16(mgDf50)*, JK1438 *daf-2(m65)/qC1*, JT193 *daf-2(sa193)*, JT6723 *daf-2(sa223)/qC1*, NS3227 *daf-18(nr2037)*, and TJ356 *zIs356* [*daf-16::GFP rol-6(su1006)*]. *daf-2(m631)* and *daf-2(m646)* were isolated during an EMS screen for nonconditional Daf-c mutants (I. Caldicot and D. L. Riddle, personal communication). *daf-2(tm1236)* was generated on request by the National Bioresource Project (Tokyo) (http://shigen.lab.nig.ac.jp/c.elegans/).

Strain constructions: The many multiple mutants created for this study were prepared using standard strain construction methodologies (details available on request from the authors). In construction of all *daf-2; daf-18* and *daf-16; daf-2* strains involving nonconditional *daf-2* alleles, the presence of each mutation was confirmed either by PCR product size or by DNA sequencing. The primers used for PCR to test for the presence of the deletions were as follows: for *daf-16(mgDf50)*—daf-16F1, gccactttattggaatttgagc; and daf-16R1, atcctcccata gaaggaccatt [PCR from gDNA with this primer pair yields a product with *daf-16*(+) but not *mgDf50*]; for *daf-18(nr2037)*—F3, gattggtgtctacgtggaacgg; or F6, ctattgaaggaggactaacacaggc, and R3, gccaacgaagtgctaaatcgac [PCR with F3 and R3 amplifies a 0.8-kb fragment only from *daf-18*(+) gDNA; F6 and R3 amplify 0.6- and 1.6-kb fragments from *nr2037* and *daf-18* (+) gDNA], respectively (Mihaylova *et al.* 1999); for *daf-2 (tm1236)*—F16F, ctggaccggaagccgaatcc; and Ex14F2A, tgac gattcagaagcactgg. In *daf-2*(+), these primers generate a product of 1.1 kb, and in *daf-2(tm1236)*, they generate a product of 0.6 kb.

Sequencing of mutant alleles: The entire coding sequence of the *daf-2* transcript was amplified as a series of overlapping fragments by RT–PCR. These fragments were then sequenced on both strands; most fragments were sequenced twice, giving fourfold coverage of the region. Sequence was compared to the wild-type sequence reported by Kimura *et al.* (1997) (GenBank AF012437) and the sequence of the *daf-2* predicted gene in WormBase (GenBank NM065249). Fragments that contained identical nucleotide substitutions on both strands compared to the wild-type sequences were taken to be the mutation in the allele. This region was then amplified from genomic DNA isolated from the mutant worms and sequenced to confirm the presence of the lesion.

Differences in the wild-type DAF-2 sequence: The sequence of the mutant cDNA was translated *in silico* and then compared to the reported wild-type DAF-2 protein sequences to determine the amino acid change. The two wild-type DAF-2 sequences (Kimura *et al.* 1997 and WormBase) differ in length by three amino acids (1846 aa *vs.* 1843 aa); the residues Met–Thr–Arg at the N terminus of the Kimura *et al.* (1997) sequence are not present in the WormBase sequence, which uses the second in-frame ATG codon as the start of translation. We chose to use the numbering system of Kimura *et al.* (1997) for the position of the mutations identified in this study. This protein sequence also differs from the WormBase protein sequence at two positions. In the Kimura *et al.* (1997) DAF-2 sequence, Arg and Gln residues occupy positions 838 and 1313, respectively. In the WormBase DAF-2 sequence, His and Lys residues occupy the equivalent positions. Our DAF-2 sequence proved to be the same as the WormBase sequence.

Irregularities with daf-2 alleles: The *e979* allele was previously reported to have a G383E substitution in the cysteine-rich (CR) domain of the DAF-2 receptor (Scott *et al.* 2002). However, the *m41* allele has also been reported to contain this mutation (Yu and Larsen 2001). The *m41* allele is class 1 and *e979* is class 2 and the Daf-c phenotype of *e979* is more severe than that of *m41* (Gems *et al.* 1998). We sequenced and phenotyped our lab stock of *daf-2(e979)* and resequenced and phenotyped the *e979* allele used by Scott *et al.* (2002) and found that the mutation in our lab stock of *e979* was C146Y,

TABLE 1

***daf-2* allele class-specific epistasis and traits**

	daf-2 allele													
	Class 1									Class 2				
Interacting mutation/treatment	*e1371*	*e1368*	*e1365*	*m577*	*sa193*	*m596*	*m41*	*m212*	*e1369*	*m579*	*e1370*	*e1391*	*e979*	Source
						Daf-c/larval arrest								
daf-12(m20)	—	—	S	S	S	S	S	S	S	—	E	E	C	Gems *et al.* (1998)
din-1S(dh127)	—	S	—	—	—	—	—	—	S	—	N[a]	N[a]	—	Ludewig *et al.* (2004)
Δ^4-dafachronic acid	—	S	—	—	—	—	—	—	—	—	(S)	—	—	Motola *et al.* (2006)
rop-1(pk93)	—	—	—	—	—	(S)	(S)	—	—	E	E	—	—	Labbé *et al.* (2000)
soc-1(n1789)	—	—	—	S	—	—	—	—	—	—	(S)	—	—	Hopper (2006)
						Age								
daf-12(m20)	—	—	(S)	(S)	(S)	—	(S)	N	—	—	E	E	E	Gems *et al.* (1998)
soc-1(n1789)	—	—	—	N	—	—	—	—	—	—	E	—	—	Hopper (2006)
daf-9(rh50)	—	(S)	—	—	—	—	—	—	—	—	(S)/E[b]	—	—	Gerisch *et al.* (2001)
Whole gonad ablation	—	N	—	—	—	E	E	—	—	—	E	—	—	Hsin and Kenyon (1999)
Hyp phenotype[c]	SH	SH	SH	SH	—	+	+[d]	—	+	++	++	+	—	Scott *et al.* (2002)

daf-2 alleles are listed in approximate order of increasing severity of the Daf-c phenotype within each allele class. S, full suppression. (S), partial suppression. E, enhancement. N, little effect. C, complex interaction. —, not determined.

[a] Tested for suppression, but not for enhancement.

[b] Weakly suppressed at 15°, enhanced at 22.5°.

[c] SH, sensitive to hypoxia. +, resistant to hypoxia, but >10% death. ++, <10% death under hypoxia.

[d] Identified in Scott *et al.* (2002) as *e979* (C. M. Crowder, personal communication). This mistake was due to the *m41* allele being misidentified as *e979* when initially sent from the Gems laboratory to the *Caenorhabditis* Genetics Center. Only class 2 alleles show a high level of resistance to hypoxia.

which affects the L1 domain. This stock exhibited a phenotype as previously reported (Gems *et al.* 1998). Sequencing of the *e979* allele used by Scott *et al.* (2002) confirmed the G383E substitution in this strain. Phenotypic analysis confirmed that this strain was actually *m41* and not *e979*. Scott *et al.* (2002) obtained the stock from the *Caenorhabditis* Genetics Center, which initially had an *m41* stock that was misidentified as *e979*. This error was corrected in September 2002.

Oligonucleotide array analysis: Microarray analysis of sterile, 1-day-old adults of the genotypes *glp-4(bn2); daf-2(m577)*, *glp-4(bn2); daf-2(e1370)*, *glp-4(bn2) daf-16(mgDf50); daf-2(m577)*, and *glp-4(bn2) daf-16(mgDf50); daf-2(e1370)* was described previously (McElwee *et al.* 2004). In that study, for each genotype examined, five biological replicates were performed, and data for the two alleles of *daf-2* were pooled. For this study, this data set was reanalyzed using newer methods, and the two alleles were treated separately, generating lists of genes that are differentially expressed in each allele.

Raw microarray data (cel files) were normalized, fold-changes between genotypes were determined, and global statistical analysis was performed, using a slightly modified version of the recently described "Goldenspike" methodology implemented in R (version 2.0.1) (Choe *et al.* 2005) (http://www.r-project.org/). Briefly, this procedure performs eight different normalization routines, which are then used to produce an average fold-change difference and false-discovery rate (q-value) between different genotypes that takes into consideration the variance of probe set intensity across the different normalizations. The Goldenspike methodology has been shown to out-perform most commonly used normalization methods (Choe *et al.* 2005). The Goldenspike protocol was altered slightly to exclude absent probe sets (those probe sets called "absent" in all hybridizations by MAS5) prior to the final probe-set-level Loess normalization. This alteration was found to reduce the number of false positives associated with the absent probe sets (Schuster *et al.* 2007).

Life-span measurements: Animals were raised at 15° and shifted to 22.5° at the L4 stage. In measures of life span, day 0 is the L4 stage. In most trials, the inhibitor of DNA replication fluorodeoxyuridine (FUdR) was added to plates (Gandhi *et al.* 1980) to prevent death due to internal hatching of eggs.

Microscopy: For Nomarski (differential interference contrast) imaging of nematodes, we used a Leica RXA2 compound microscope, with a Hamamatsu Orca-ER B/W CCD digital camera.

RESULTS

Incomplete suppression of severe *daf-2* mutations by *daf-18(0)* and *daf-16(0)*: We began by characterizing four nonconditional *daf-2* alleles: *m65*, *m631*, *m646*, and *tm1236*. In each case, homozygous *daf-2* segregants from balanced *daf-2*/+ hermaphrodites form dauer larvae nonconditionally (data not shown). We performed epistasis tests, initially with *m65*, *m631*, and *m646*, and the dauer defective, suppressor mutations *daf-18(nr2037)* and *daf-16(mgDf50)*, both of which are putative null alleles. The *nr2037* mutation is a 990-bp deletion in *daf-18*, which results in loss of critical elements of the gene product (Gil *et al.* 1999; Mihaylova *et al.* 1999); *mgDf50* is a deletion that removes most of the *daf-16* coding region (Ogg *et al.* 1997). Here the aims were to reveal differences in severity among nonconditional *daf-2* alleles to identify potential *daf-2* null alleles and to understand interactions among *daf-2*, *daf-18*, and *daf-16*.

TABLE 2

Incomplete suppression of nonconditional Daf-c alleles of *daf-2* by *daf-16* and *daf-18*

Genotype	% L4 adults	% L1, L2[a]	% dauer	% dead eggs	*N*
		At 25°			
+	99	0	0	1	295
daf-18(nr2037)	100	0	0	0	275
daf-16(mgDf50)	100	0	0	0	325
daf-2(m65)	—	—	92	—	1361[b]
daf-2(m65); daf-18	24	6	0	70	171
daf-2(m631); daf-18	67	26	0	7	85
daf-2(m646); daf-18	92	5	0	3	283
daf-16; daf-2(m65)	0	0	0	100	298
daf-16; daf-2(m646)	100	0	0	0	172
		At 15°			
+	99	0	0	1	230
daf-18	100	0	0	0	189
daf-16	100	0	0	0	257
daf-2(m65); daf-18	65	6	5	24	109
daf-2(m631); daf-18	78	0	22[c]	0	172
daf-2(m646); daf-18	89	0	11[c]	0	221
daf-16; daf-2(m65)	43	18	0	39	292
daf-16; daf-2(m646)	100	0	0	0	210

[a] These larvae are morphologically abnormal at 25°, but not at 15°.

[b] Data were derived from Gems *et al.* (1998). Seventy-five percent of segregants from *m65*/+ mothers reached adulthood, 23% formed dauers, and the remainder were a mixture of dead eggs, L1's, or unhealthy, clear-looking arrested L2's.

[c] Partial dauers, recovered within 24 hr.

daf-18 encodes a PTEN phosphatase, which is a negative regulator of signaling via DAF-2 and AGE-1 (Ogg and Ruvkun 1998; Gil *et al.* 1999; Mihaylova *et al.* 1999; Rouault *et al.* 1999). *PTEN* (phosphatase and tensin homolog deleted on chromosome 10) is a commonly mutated tumor suppressor gene in human cancer. PTEN phosphatases attenuate insulin/IGF-1 signaling by dephosphorylating phosphatidylinositol 3,4,5-trisphosphate (PIP_3) on position 3 of the inositol ring. *daf-18(nr2037)* fully suppresses both the Daf-c and Age phenotypes of *daf-2(e1370)* (Gil *et al.* 1999; Mihaylova *et al.* 1999). Thus, it is thought that DAF-2 acts principally by stimulating PIP_3 production and by inhibiting DAF-16 activity (Kenyon *et al.* 1993; Riddle and Albert 1997; Mihaylova *et al.* 1999).

At 25°, *daf-18* fully suppressed Daf-c in *m631* and *m646*, but also resulted in 33 and 8% early developmental arrest, respectively (Table 2). This implies that *m631* is the more severe allele. In the case of *daf-2(m65); daf-18* double mutants, a high proportion of animals arrested development as embryos. At 15°, all three *daf-2; daf-18* strains showed some dauer-like arrest at a low frequency (Table 2). This cold-sensitive Daf-c trait implies that the *daf-18* mutation is temperature sensitive in its effects. Given that *daf-18(nr2037)* is a nullimorphic allele, this

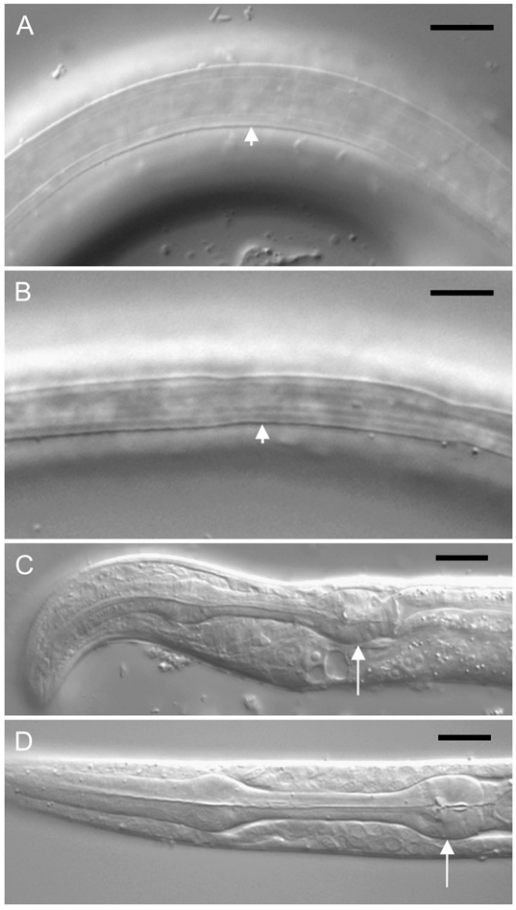

FIGURE 1.—Combined effects of severe *daf-2* alleles and *daf-18(nr2037)* or *daf-16(mgDf50)* on development. (A) Cuticle of *daf-2(m646); daf-18(nr2037)* dauer-like larva showing L3 ala (short arrow). (B) Cuticle of *daf-2(m65); daf-18(nr2037)* dauer larva showing dauer ala (short arrow). (C) Anterior end of morphologically abnormal *daf-2(m631); daf-18(nr2037)* L1 larva, showing hypertrophy of ventral side of the head and dorsal displacement of pharynx (long arrow). (D) Anterior end of morphologically normal wild-type L1 larva (long arrow). Bars, 10 μm.

could imply the presence of a second PIP_3 phosphatase that is functionally redundant with DAF-18, but only at lower temperatures. In the case of *m631* and *m646*, these arrested larvae were partial dauers with dark, radially contracted bodies, yet there were also non-dauer alae (Figure 1A) and some pharyngeal pumping. These larvae resumed development after several days. By contrast, *daf-2(m65); daf-18* dauers appeared fully differentiated and resumed development only after ~1 week. Under the dissecting microscope these animals resembled normal dauer larvae with dauer alae (Figure 1B) and no pharyngeal pumping in most cases. Some arrested embryos were also present. These results demonstrate the following order of decreasing mutant allele severity: *m65* > *m631* > *m646*.

Severe *daf-2* alleles causing nonconditional dauer arrest have previously been combined with reduction-of-function alleles of *daf-16* (GOTTLIEB and RUVKUN 1994; LARSEN *et al.* 1995). In *daf-2(mg43)*, (nonconditional) Daf-c is suppressed by *daf-16(m27)* at 25° (GOTTLIEB and RUVKUN 1994). The nonconditional Daf-c phenotype of *daf-2(m65)* was also suppressed by the reduction-of-function allele *daf-16(m26)* at 15°; however, at 25.5°, the double mutant was embryonic lethal (LARSEN *et al.* 1995). We examined the developmental effects of *daf-16(mgDf50)* on *daf-2(m65)* and *daf-2(m646)*. In both *daf-2* alleles, dauer formation was fully suppressed at 15° and in *m646* at 25° (Table 2). In the case of *daf-16(mgDf50); daf-2(m65)* at 25°, 100% embryonic arrest occurred, similar to previous observations of *daf-16(m26); daf-2 (m65)* (LARSEN *et al.* 1995). In addition, *daf-16(mgDf50); daf-2(tm1236)* animals developed normally at 25°, demonstrating that *tm1236* is a weaker allele than *m65* (data not shown).

daf-2; daf-18 and *daf-16; daf-2* mutants exhibited a range of other mutant phenotypes. All three *daf-2; daf-18* strains and *daf-16; daf-2(m65)*-arrested first-stage larvae exhibited variable and sometimes severe morphological abnormalities, including ventral swelling in the region of the terminal bulb of the pharynx, resulting in dorsal displacement of the pharynx (Figure 1, C and D) and, in some cases, kinks in the anterior intestine. In this region, disorganization of the cuticular alae was sometimes seen. A small proportion of adult animals also showed a weak uncoordinated phenotype, with reduced movement, and a tendency to kink behind the pharynx when backing. These defects suggest that insulin/IGF-1 signaling plays a role in morphogenesis and early development.

Nonconditional *daf-2* alleles and aging: We tested the requirement for *daf-18* and *daf-16* gene function of the *daf-2* life extension (Age) phenotype in severe *daf-2* mutants. By itself, *daf-18(nr2037)* shortened life span relative to wild type, as previously seen. The Age phenotype of the weak mutant *daf-2(e1370)* was largely, but not fully, suppressed by *daf-18* (Table 3). Consistent with their greater loss of function, *m65*, *m631*, and *m646* all resulted in larger increases in life span when added to *daf-18*. In two of three trials, *daf-2(m65); daf-18* animals were also longer lived than wild-type controls. In a direct comparison of *daf-2; daf-18* strains (Table 3, trial 4), *daf-2(m65); daf-18* animals were longer lived than *daf-2 (m631); daf-18* animals ($P < 0.0001$, log rank test), and *daf-2(m631); daf-18* than *daf-2(m646); daf-18* ($P = 0.03$). The implied order of mutant severity is consistent with that inferred from effects on development. Given its relative phenotypic severity and molecular identity, *daf-2 (m65)* is a strong candidate for a null allele.

We examined the requirement for *daf-16* gene function of the *daf-2* life extension (Age) phenotype in three severe *daf-2* alleles: *m646*, *m65*, and *tm1236*. In no case was the life span of *daf-16(mgDf50); daf-2* animals consistently different from that of *daf-16* alone (Table 3). Thus, the effect of *daf-2* on aging is fully dependent on *daf-16*.

TABLE 3

Effects of *daf-2*, *daf-18*, and *daf-16* on life span

Genotype	Mean (days) ±SE	Median (days)	Maximum (days)	N^a	P^b	P^c
			Trial 1			
+	15.5 ± 0.5	15	22	55 (84)	—	—
daf-18(nr2037)	8.2 ± 0.3	7	13	63 (102)	<0.0001	—
daf-16(mgDf50)	10.6 ± 0.3	9	17	68 (80)	<0.0001	—
daf-2(e1370)	29.9 ± 2.4	35	42	21 (77)	<0.0001	—
daf-2(e1370); daf-18(0)	9.9 ± 0.3	10	13	77 (94)	<0.0001	<0.0001
daf-2(m646); daf-18(0)	13.2 ± 0.4	13	21	79 (102)	<0.0083	<0.0001
daf-16(0); daf-2(m646)	9.8 ± 0.3	9	16	84 (84)	<0.0001	0.1423
			Trial 2			
+	16.2 ± 0.5	18	21	62 (75)	—	—
daf-18(nr2037)	9.2 ± 0.1	10	10	87 (100)	<0.0001	—
daf-16(mgDf50)	11.2 ± 0.1	11	11	100 (100)	<0.0001	—
daf-2(m65); daf-18(0)	[d] 8.2 ± 0.5	7	14	72 (75)	<0.0001	0.6757
daf-16(0); daf-2(m65)	9.7 ± 0.4	11	14	95 (98)	<0.0001	0.6486
			Trial 3			
+	16.3 ± 0.6	16	26	60 (60)	—	—
daf-18(nr2037)	10.4 ± 0.3	12	14	89 (100)	<0.0001	—
daf-16(mgDf50)	13.4 ± 0.2	14	14	93 (100)	<0.0001	—
daf-2(m65); daf-18(0)	28.9 ± 0.5	29	37	95 (100)	<0.0001	<0.0001
daf-16(0); daf-2(m65)	14.2 ± 0.2	14	16	97 (100)	<0.0001	<0.0002
			Trial 4			
+	13.4 ± 0.3	13	17	72 (75)	—	—
daf-18(nr2037)	8.4 ± 0.2	10	11	77 (100)	<0.0001	—
daf-2(m65); daf-18(0)	17.6 ± 0.6	17	26	90 (100)	<0.0001	<0.0001
daf-2(m631); daf-18(0)	14.9 ± 0.3	17	19	90 (100)	<0.0001	<0.0001
daf-2(m646); daf-18(0)	13.6 ± 0.3	14	14	96 (100)	0.0284	<0.0001
			Trial 5			
+	19.4 ± 0.4	18	28	99 (100)	—	—
daf-16(mgDf50)	12.9 ± 0.1	12	16	100 (100)	<0.0001	—
daf-16(0); daf-2(m65)	12.3 ± 0.3	12	20	90 (100)	<0.0001	0.3922
daf-16(0); daf-2(m646)	12.2 ± 0.1	12	14	99 (100)	<0.0001	<0.0001
daf-16(0); daf-2(tm1236)	12.4 ± 0.1	12	16	96 (100)	<0.0001	0.0041
			Trial 6			
+	16.2 ± 0.2	16	20	98 (100)	—	—
daf-16(mgDf50)	12.2 ± 0.1	12	16	99 (100)	<0.0001	—
daf-16(0); daf-2(m65)	11.1 ± 0.3	12	18	96 (100)	<0.0001	0.0552
daf-16(0); daf-2(m646)	12.2 ± 0.2	12	20	99 (100)	<0.0001	0.5758
daf-16(0); daf-2(tm1236)	12.6 ± 0.1	12	16	96 (100)	<0.0001	0.0138

FUdR was used for trials 2–4 to prevent death due to internal hatching of eggs, which affected some of the double-mutant strains. Maximum life span is the last day on which live worms were observed.

[a] Deaths scored (initial sample size).

[b] Probability that life span is identical to that of wild type with same temperature history (log rank test).

[c] Probability that life span is identical to that of single Daf-d mutant (log rank test).

[d] In trial 2, *daf-2(m65); daf-18(0)* is not longer lived than *daf-18(0)*, in contrast to trials 3 and 4. While the reason for this discrepancy is unknown, we believe that the latter results are correct, given that *daf-2(m631)* and *daf-2(m646)* also increase *daf-18(0)* life span and that the severity ranking of the effects of these three *daf-2* alleles is the same for both life span and larval arrest.

In humans, many mutations affecting the insulin receptor are semidominant (Taylor *et al.* 1992). This may reflect wild-type proreceptors combining with mutant proreceptors to form nonfunctional receptor dimers. By contrast, the life span of *daf-2/+* hermaphrodites using the most severe *daf-2* allele, *m65*, was not increased relative to wild-type controls (two trials at 22.5°; data not shown). Thus, in contrast to the mammalian

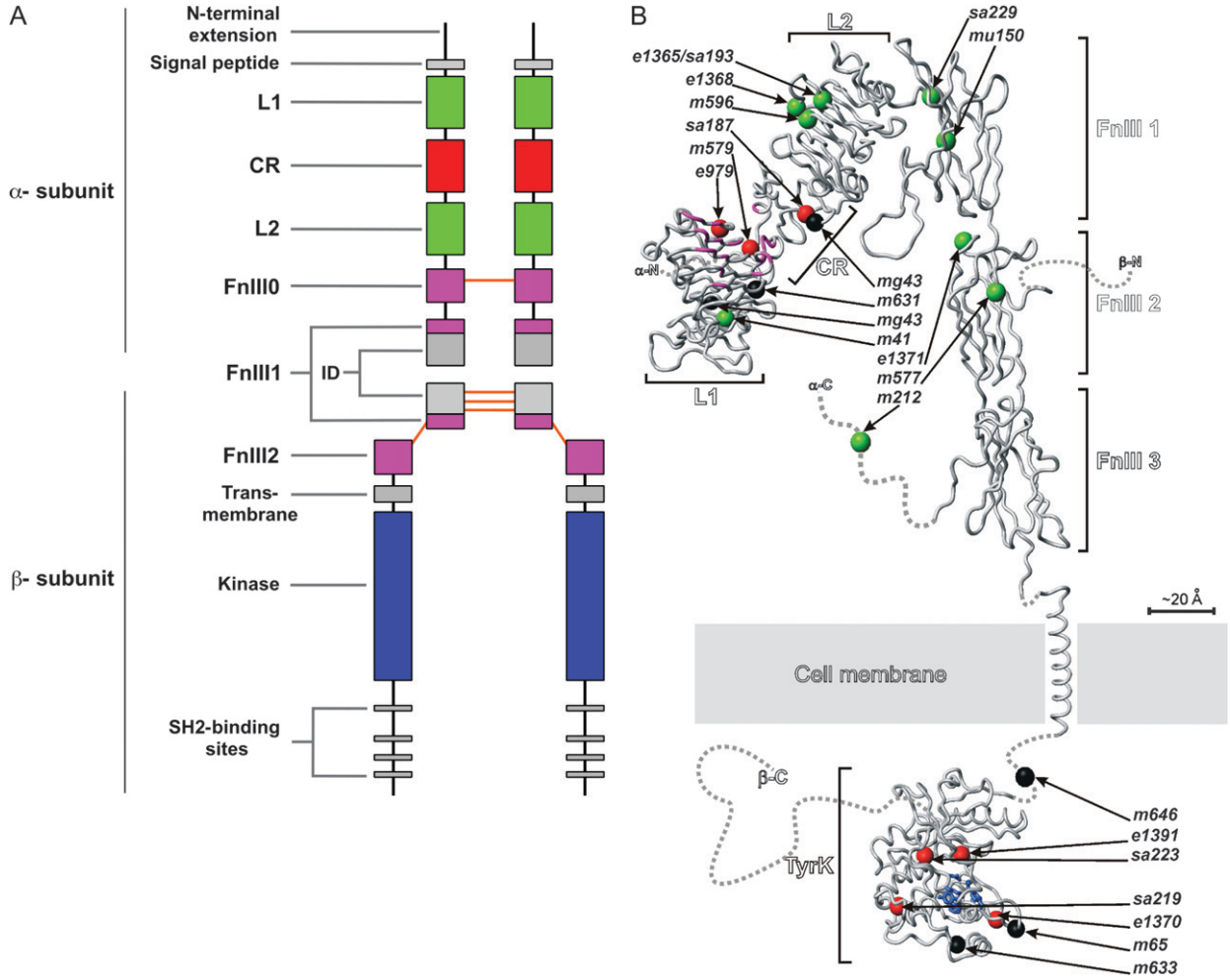

FIGURE 2.—Position and nature of mutant lesions affecting the DAF-2 protein. (A) DAF-2 domain structure. The N-terminal extension and signal peptide are predicted to be cleaved off during processing of the proreceptor. The C-terminal extension is the region C-terminal of the kinase domain. The orange lines represent cysteine residues involved in interchain disulfide bonds. The α- and β-subunits of each heterodimer are linked by a predicted bond between C827, located in the insert domain of FnIII2, and C1126, located within the FnIII3 domain. The holoreceptor is formed by disulfide bonds between equivalent cysteines in adjacent α-subunits at positions C706 (FnIII1), C882, C883, and C886 (insert domain of FnIII2). (B) Backbone representation of homology models of the domains of DAF-2, showing the location of the mutations in the alleles studied. Green, class 1 mutations; red, class 2 mutations; black, nonconditional mutations. The regions of L1 and CR that are thought to interact with human IGF-1 and/or Ins are in purple (note the clustering of class 2 and nonconditional mutations in this region). The active site of the tyrosine kinase domain is in blue. Dashed lines represent regions that are intrinsically unfolded or without known structure. The model was constructed using the atomic coordinates of the extracellular domain of hInsR (PDB code: 2DTG) and the kinase domain of hInsR (PDB code: 1IRK).

insulin receptor, mutations affecting the DAF-2 receptor appear to be fully recessive.

Sequence analysis of nonconditional *daf-2* alleles: DNA sequencing was used to identify the mutant lesions in the nonconditional alleles. Three are nonsense alleles: *m65* (W1449*, amber), *m631* (R281*, opal), and *m646* (Q1223*, ochre) (Figure 2B, Table 4). Although *m65* is phenotypically the most severe allele, it is predicted to result in the least truncated protein (see DISCUSSION). W1449 is in the tyrosine kinase domain and the region following it is necessary for kinase function, so *m65* is predicted to result in a truncated receptor without kinase activity. *tm1236* contains an in-frame 561-bp deletion in exon 14, which is predicted to result in a Y1234S substitution and the loss of 187 amino acids, 1235–1421, from the kinase domain. This deletion removes the catalytic and activation loops of the kinase domain, but leaves intact the unusual C-terminal extension that DAF-2 possesses.

Analysis of conditional alleles of *daf-2*: Next, we conducted an analysis and survey of conditional *daf-2* alleles. Our overall aim was to build up a more detailed picture of the phenotypic range of *daf-2* mutants and to understand it in terms of genotype and of changes in receptor structure and function. We first probed the difference in terms of DAF-16 function and gene expression between *daf-2(m577)*, a class 1 allele, and *daf-2 (e1370)*, a class 2 allele.

TABLE 4

Mutant lesions in *daf-2* alleles

Allele	Class[a]	Mutation location location (domain)	DNA change	Amino acid change	Reference	Predicted outcome of mutation[b]
e979	2D	L1	TGC-TAC	C146Y	This study	a
m631	NC	L1	CGA-TGA	R281STOP	This study	b
m41	1B	Cys-Rich	GGA-GAA	G383E	Yu *et al.* (2002)	c
mg43[c]	NC	Cys-Rich	TGT-TAT	C401Y	Kimura *et al.* (1998)	a
m579	2B	Cys-Rich	CGT-TGT	R437C	Scott *et al.* (2002)	d, h, i
sa187	2C	Cys-Rich	TGT-AGT	C469S	Kimura *et al.* (1998)	a
mg43[c]	NC	Cys-Rich	CCC-CTC	P470L	Kimura *et al.* (1998)	d
m596[d]	1E	L2	GGC-AGC	G547S	Scott *et al.* (2002)	e, h
e1368	1A	L2	TCA-TTA	S573L	Kimura *et al.* (1998)	e
e1365/sa193[e,f]	1A	L2	TGC-TAC	A580T	Kimura *et al.* (1998); this study	f
sa229	1A	FnIII1	GAT-AAT	D648N	Kimura *et al.* (1998)	g
mu150	1A	FnIII1	GGC-GAC	G682D	This study	f
e1371	1A	FnIII2α	GGA-GAA	G803E	This study	d
m212	1D	FnIII2ID	TGT-TAT	C883Y	This study	a, h
m577[f]	1C	FnIII2β	TGC-TAC	C1045Y	This study	a, h
m646	NC	Prekinase	CAA-TAA	Q1223STOP	This study; K. Kimura and G. Ruvkun (personal communication)	b
sa219	2C	Kinase	GAT-AAT	D1374N	Kimura *et al.* (1998)	d
sa223	2E	Kinase	CGA-CAA	R1430Q	This study	d, h, i
e1391	2D	Kinase	CCC-CTC	P1434L	Kimura *et al.* (1998)	d, i
m65	NC	Kinase	TGG-TAG	W1449STOP	This study	b
e1370	2C	Kinase	CCA-TCA	P1465S	Kimura *et al.* (1998)	d
m633	NC	Kinase	CGT-CAT	R1510H	K. Kimura and G. Ruvkun (personal communication)	d
tm1236	NC	Kinase	Deletion (see text)		This study	

[a] Classes as defined in Gems *et al.* (1998). NC, nonconditional Daf-c.

[b] a: Residue affected is a disulfide-bonded cysteine. Substitution is likely to disrupt fold stability. b: Nonsense mutation implying truncation of the polypeptide chain. Mutant protein is expected not to be functional. c: Residue affected is in a part of the sequence present only in nematodes. We were unable to predict the effect of substitution on the basis of homology to mammalian receptors. d: Residue affected is highly conserved in all phyla. Substitution is likely to affect stability of the structure or aspects of the receptor mechanism. e: Residue affected is solvent inaccessible and not highly conserved across phyla. The conservative nature of the substitution means that it is not predicted to have major detrimental effects. f: Residue affected is solvent inaccessible and not highly conserved across phyla. The nonconservative nature of the substitution suggests that it is likely to disrupt fold stability. g: Residue affected is solvent accessible and not highly conserved across phyla. Currently unable to predict effect of substitution. h: A nonidentical, naturally occurring, or engineered mutation in the equivalent *h*InsR position has been reported. i: An identical, naturally occurring, or engineered mutation in the equivalent *h*InsR position has been reported. For further details, see http://www.biochem.ucl.ac.uk/rilm.

[c] The *mg43* allele has two lesions, both affecting the CR domain.

[d] Previously defined as class 2A (Gems *et al.* 1998). Given that this allele is suppressed by *daf-12(m20)*, we have redesignated it as a class 1 allele.

[e] The *e1365* and *sa193* alleles were isolated in different labs but contain identical sequence changes.

[f] Sequence analysis revealed that the allele identified as *e1365* in Gems *et al.* (1998) was in fact *daf-2(m577)*. The real *e1365* (Kimura *et al.* 1997) is a class 1A allele.

Allele differences in effects on DAF-16 localization: *daf-2(e1370)* results in loss of cytoplasmic retention of the DAF-16 transcription factor and its concentration in the nucleus (Henderson and Johnson 2001; Lee *et al.* 2001; Lin *et al.* 2001). We compared nuclear localization of GFP-tagged DAF-16 in *daf-2(m577)* and *daf-2(e1370)* mutant backgrounds. In *daf-2(e1370)* animals raised at 15° and shifted as L3 larvae to 25° for 4 hr, full nuclear localization was seen (Figure 3B). By contrast, under the same conditions, no nuclear localization was seen in *daf-2*(+) or *daf-2(m577)* animals (Figure 3, A and C). After 24 hr at 25°, and more so after 48 hr, a small degree of nuclear localization was visible in *daf-2(m577)* but not in *daf-2*(+) adults (not shown). In *daf-2(e1370)* adults raised and maintained at 15°, weak nuclear localization was observed (Figure 3D). This implies greater activation of DAF-16 in *daf-2(e1370)*.

We then asked whether this difference in DAF-16::GFP localization is typical of class 1 *vs.* class 2 alleles by examining four more *daf-2* alleles: *m41* (weak class 1), *m212* (severe class 1), *m579* (weak class 2), and *e979* (severe class 2). The pattern of DAF-16::GFP localization was the same in *m41* as *m577* and in *m579* as *e1370* (data not shown). Unfortunately, in the case of *m212*

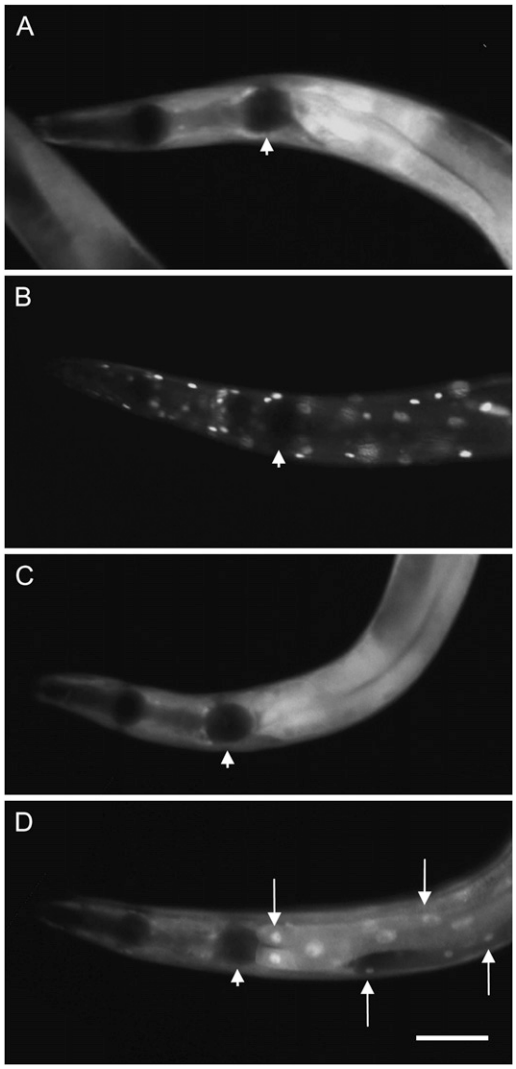

Figure 3.—Effects of two *daf-2* mutations on DAF-16 localization. (A) *daf-2*(+) at 25°. (B) *daf-2(e1370)* at 25°. (C) *daf-2 (m577)* at 25°. (D) *daf-2(e1370)* at 15°. Anterior of animal to the right. Arrows indicate nuclear localization of DAF-16::GFP. Arrowheads indicate position of the grinder of the pharynx. Bar, 50 μm.

and *e979*, the presence of the *daf-16::gfp* transgene caused nonconditional dauer formation. These results suggest that DAF-16 is typically more active in weak class 2 alleles than weak class 1 alleles. It is notable that DAF-16 showed little nuclear localization in *m41* despite the fact that in terms of Daf-c it is a more severe allele than *e1370*.

***daf-16*-dependent differences in gene expression in *daf-2(m577)* and *daf-2(e1370)* mutants:** The different effects of *daf-2* alleles on DAF-16 localization may differentially affect DAF-16-mediated gene expression, which could contribute to phenotypic differences among *daf-2* mutants. To explore this, we used whole-genome oligonucleotide microarrays (Affymetrix) to compare DAF-16-dependent transcription in *daf-2(m577)* and *daf-2(e1370)*. An analysis of summed data from these two alleles has been described previously (McElwee *et al.* 2004). Our expectations were that in *daf-2(e1370)* there would be more differentially expressed genes, on the basis of the greater nuclear localization of DAF-16, and also the additional mutant phenotypes of class 2 *daf-2* mutants (Gems *et al.* 1998). Comparisons were made between *daf-2* (long lived, DAF-16 ON) and *daf-16(mgDf50); daf-2* (not long lived, DAF-16 OFF) for *daf-2(m577)* and *daf-2(e1370)* (five biological replicates per genotype). Reproduction was blocked using the *glp-4(bn2*ts*)* mutation, and age-synchronized young adults were studied (McElwee *et al.* 2004).

We identified genes (represented by probe sets on the oligonucleotide arrays) where transcript abundance is significantly different between *daf-2* and *daf-16; daf-2* ($q < 0.1$). There were 1252 and 581 such probe sets for *daf-2(m577)* and *daf-2(e1370)*, respectively, including 356 probe sets in common. The smaller number of genes with altered expression in *daf-2(e1370)* was unexpected, but is likely to reflect greater variance observed in gene expression in *daf-2(e1370)* strains. The average standard deviation of probe sets for the five replicates of each genotype, for a typical data normalization, were as follows: *daf-2(m577)*, 0.59; *daf-16; daf-2(m577)*, 0.50; *daf-2 (e1370)*, 0.75; and *daf-16; daf-2(e1370)*, 0.78.

A total of 525 genes showed a significant change in expression in *daf-2* relative to *daf-16; daf-2* for *m577* ($q < 0.1$) but not for *e1370* ($q > 0.5$) (data not shown). Although some of these genes may actually show *m577*-specific regulation, for others this may be an artifact of the difference in variance, described above. More interesting, therefore, were the 56 genes showing altered expression in *daf-2* relative to *daf-16; daf-2* for *e1370* but not for *m577* (listed in Table 5). Potentially, these genes contribute to the more pleiotropic character of *e1370* and to its epistatic interactions (Table 1).

Of the 56 genes listed here, half are upregulated and half downregulated. Among the most strongly upregulated genes are F08H9.3 and F08H9.4, which are neighboring genes regulated by distinct promoters and which encode small heat-shock proteins (smHSPs) of the HSP-16 type. Several lines of evidence implicate smHSPs in longevity assurance in *C. elegans* (Walker *et al.* 2001; Hsu *et al.* 2003; Walker and Lithgow 2003). Both F08H9.3 and F08H9.4 are constitutively expressed, the former in the pharynx and the latter in the excretory canal and ventral nerve-cord neurons (Shim *et al.* 2003). Also of note is the upregulation of *ins-22*, a neuronally expressed type α insulin-like peptide and potential ligand for DAF-2 (Pierce *et al.* 2001), and *nhr-206*, an orphan nuclear hormone receptor.

A comparison of gene expression in *daf-16(0); daf-2 (m577)* and *daf-16(0); daf-2(e1370)* strains revealed no genes showing a significant difference in expression level ($q < 0.1$). Thus, all differences in gene expression between these two alleles appear to be *daf-16* dependent.

TABLE 5

Genes showing differential expression between *daf-2* and *daf-16; daf-2* in *e1370* but not in *m577*

daf-2 vs daf-16; daf-2 mean $\log_2$ fold-change	*q*	Gene sequence name	Protein
			Upregulated in *daf-2*
6.13	0.000961	Y39H10A.1	Similarity to *Bradyrhizobium* sp. Hypothetical protein TR:Q35RI1
5.318	0.00204	F08H9.4	IPR002068 heat-shock protein Hsp20
3.707	0.0101	F08H9.3	IPR002068 heat-shock protein Hsp20
3.754	0.00795	*gst-41*	IPR004045 glutathione S-transferase, N-terminal
3.572	0.0276	T20D4.12	IPR002542 protein of unknown function DUF19
3.48	0.0209	F20A1.6	Similarity to *Dictyostelium discoideum* TR:Q55ED2
3.417	0.00252	*cyp-13B1*	IPR001128 cytochrome P450
3.22	0.0233	C45G7.3	Similarity to Interpro domain IPR008597 (Destabilase)
3.07	0.0732	F46F5.15	Similarity to *Saccharomyces cerevisiae* GAP; negatively regulates RAS
3.03	0.0414	*tyr-3*	Predicted tyrosinase
2.982	0.00838	T20G5.8	IPR003582 metridin-like ShK toxin
2.908	0.0514	C34B2.4	IPR001781 LIM, zinc binding
2.852	0.0126	*ins-22*	IPR004825 insulin/IGF/relaxin
2.823	0.0749	F35E8.6	IPR003582 metridin-like ShK toxin
2.81	0.0734	F09E10.10	Probable noncoding RNA
2.77	0.0621	W08A12.4	Similarity to *Oryctolagus cuniculus* trichohyalin; SW:P37709
2.73	0.0317	F36D1.7	Similarity to *Clostridium cellulovorans* hydrophobic protein A
2.71	0.0480	C08A9.3	Similarity to *Mus musculus* SID1; SW:Q8CIF6
2.645	0.0611	F49E11.6	IPR001283 allergen V5/Tpx-1 related
2.615	0.0321	M162.5	IPR007114 major facilitator superfamily
2.54	0.0180	T23F2.4	Similarity to Pfam domain PF01679
2.38	0.0248	F19F10.3	Similarity to *Burkholderia thailandensis* TR:Q2SYY4
2.284	0.0352	Y38E10A.11	IPR009853 protein of unknown function DUF1412
2.18	0.0249	C50D2.6	Similarity to *D. melanogaster* CG9896-PA
1.97	0.0850	B0563.5	Similarity to *Desulfovibrio desulfuricans* metal-dependent phosphohydrolase
1.93	0.0433	Y43C5A.3	Similarity to *Ixodes scapularis* putative secreted salivary gland peptide
1.76	0.0669	F20A1.10	Similarity to *H. hepaticus* Seryl-tRNA synthetase
1.703	0.0731	*nhr-206*	IPR000324 vitamin D receptor
			Downregulated in *daf-2*
−7.084	0.000238	F22A3.6	IPR008597 destabilase
−3.542	0.0323	C52E2.5	IPR001810 cyclin-like F-box
−3.527	0.00422	T16G12.1	IPR001930 peptidase M1, membrane alanine aminopeptidase
−3.494	0.0216	R03G8.6	IPR001930 peptidase M1, membrane alanine aminopeptidase
−3.128	0.00234	C17H12.8	IPR003366 protein of unknown function DUF141
−2.826	0.0272	F52F10.4	IPR002656 acyltransferase 3
−2.755	0.00648	R09H10.5	IPR006582 MD
−2.653	0.00878	T01D3.6	IPR001846 von Willebrand factor, type D
−2.553	0.0176	*amt-4*	IPR010256 Rh-like protein/ammonium transporter
−2.496	0.0277	F28B4.3	IPR006209 EGF-like
−2.349	0.0173	C41A3.1	IPR008262 lipase, active site
−2.307	0.0188	K11H12.4	IPR005071 protein of unknown function DUF274
−2.297	0.025	T25B6.2	IPR002052 N-6 adenine-specific DNA methylase
−2.18	0.0252	K09C4.1	IPR007114 major facilitator superfamily
−2.055	0.0831	R193.2	IPR002035 von Willebrand factor, type A
−2.042	0.0354	*glc-1*	IPR006201 neurotransmitter-gated ion channel
−1.985	0.0415	C12D8.5	IPR005806 Rieske [2Fe-2S] region
−1.932	0.0323	*fat-7*	IPR005804 fatty acid desaturase
−1.910	0.0372	C29F7.2	IPR004119 protein of unknown function DUF227
−1.889	0.0693	*ugt-43*	IPR002213 UDP-glucuronosyl/UDP-glucosyltransferase
−1.870	0.0541	K08D8.6	IPR003366 protein of unknown function DUF141
−1.83	0.0611	C11E4.7	Similarity to *Trichodesmium erythraeum* aminotransferase, class I and II
−1.809	0.0547	*ckb-2*	IPR002573 choline/ethanolamine kinase
−1.74	0.00950	F08G5.6	IPR003366 protein of unknown function DUF141
−1.66	0.0695	C18H9.6	Similarity to *Geobacter metallireducens* replication initiation factor
−1.54	0.0482	F15E11.12	Similarity to *Wolinella succinogenes* hypothetical protein, TR:Q7MR69
−1.393	0.0947	*ugt-22*	IPR002213 UDP-glucuronosyl/UDP-glucosyltransferase
−1.117	0.0182	*asp-1*	IPR001461 peptidase A1, pepsin

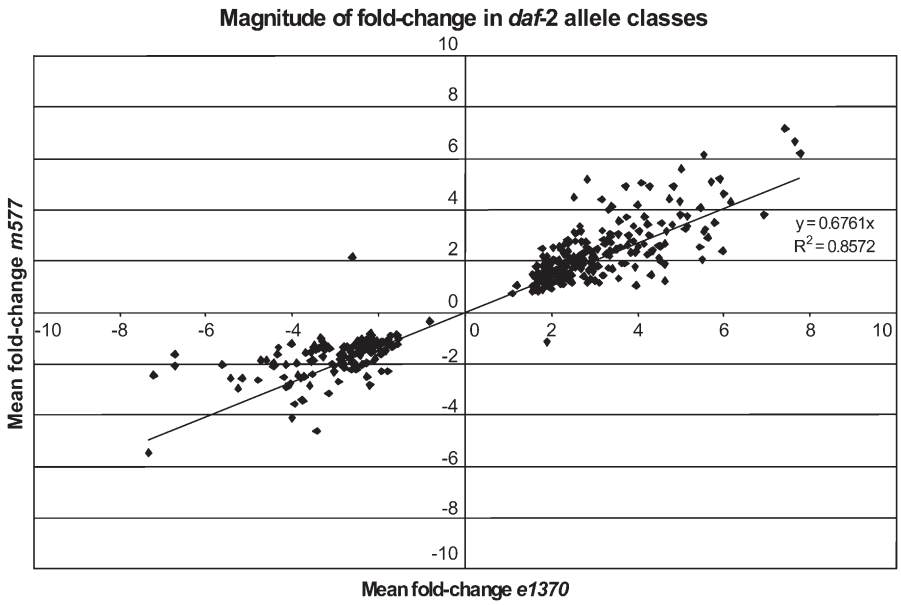

FIGURE 4.—Magnitude of mean fold-change of genes (in two alleles of *daf-2*), which showed significant ($q < 0.1$) differences in expression between *daf-2* and *daf-16; daf-2*. (356 probe sets were expressed significantly differently in both comparisons). There is a strong trend toward a greater magnitude of transcriptional change in *daf-2(e1370)* than in *daf-2(m577)*.

Next we performed a global comparison between *m577* and *e1370* of the magnitude of mean fold-change of genes that showed significant ($q < 0.1$) differences in expression between *daf-2* and *daf-16; daf-2* (Figure 4). There is a clear trend toward a greater magnitude of transcriptional change in *daf-2(e1370)* than in *daf-2 (m577)*. Taken together, these studies of DAF-16 localization and transcript abundance support the view that in *daf-2(e1370)* there is a lower level of insulin/IGF-1 signaling, leading to more nuclear localization of DAF-16 and greater DAF-16-dependent changes in gene expression.

Sequencing of eight more *daf-2* alleles: To gain further insight into the basis of *daf-2* allele differences, we sequenced eight more *daf-2* alleles that have been studied previously (GEMS *et al.* 1998; GARIGAN *et al.* 2002; MURPHY *et al.* 2003; NANJI *et al.* 2005): *e979*, *sa193*, *mu150*, *e1371*, *m212*, *m577*, *sa223*, and *e1369*. Apart from *e1369*, the lesions were identified for all alleles (Figure 2B, Table 4). *e1369* is an unusual allele, exhibiting a severe ts Daf-c phenotype, yet suppressed by *daf-12*. Although we verified that *e1369* fails to complement *daf-2(m577)* and maps very close to the *daf-2* locus at −9.61 ± 0.27, we found no mutation in the coding sequence in the 5.4-kb first intron or in the first 5.2 kb upstream of the putative translational start. Possibly the *e1369* mutation lies in a distant *cis* regulatory region; however, using RT–PCR we saw no change in *daf-2* mRNA levels in this mutant (data not shown).

We applied several data-mining approaches to gain insight into the possible mode of action of 24 *daf-2* alleles (Figure 2B, Table 4). The alleles include the 11 sequenced in this study, plus 13 *daf-2* alleles sequenced previously (KIMURA *et al.* 1997; YU and LARSEN 2001; SCOTT *et al.* 2002). First, we looked at the predicted effects of each mutation on homology models of the individual DAF-2 domains. Second, we surveyed reports on mutations in other insulin-like receptors for equivalent or similar changes to those in *daf-2* alleles for any phenotypic, biochemical, and/or structural information available. The resulting information was collated into an online web resource, Receptors for Insulin and Insulin-Like Molecules (RILM) (http://www.biochem.ucl.ac.uk/rilm/). Details of the construction and utilities of this resource have been reported elsewhere (GARZA-GARCIA *et al.* 2007).

Clustering of phenotypically defined classes of *daf-2* alleles: A survey of all sequenced *daf-2* alleles reveals that the site of the lesion in the receptor is a predictor of its phenotypic consequences. Class 1 mutations occur in the CR, L2, and fibronectin type III (FnIII) domains of the extracellular part of the receptor (Figure 2B). By contrast, class 2 and nonconditional alleles cluster around the ligand-binding cleft in the L1 and CR domains or in the tyrosine kinase domain. Thus, the phenotype-based class 1/class 2 distinction corresponds to classes of defect in the DAF-2 receptor protein. In the following sections, we survey *daf-2* mutations in more detail, emphasizing the more notable alleles.

Mutations in the receptor L domains and CR region: *e979* is the only conditional allele with a lesion in the L1 domain. This allele is also unique in that at 25.5° it causes 100% embryonic lethality and L1 arrest (VOWELS and THOMAS 1992; GEMS *et al.* 1998). *e979* results in a C146Y substitution. From the structure of the human receptors, this amino acid residue is predicted to be involved in an intradomain disulfide bond with C181. Given that it affects a structurally important residue, *e979* is likely to destabilize the protein fold. Possibly, the ts early arrest resulting from this mutation reflects resulting thermolability of the mutant receptor. In *h*InsR, C8 (equivalent to DAF-2 C146) is also very close

to a ligand-binding motif (Whittaker and Whittaker 2005), which is conserved in DAF-2. Thus, *e979* may affect binding of ligand to receptor. Four *daf-2* alleles have mutations in the L2 domain: *e1365*, *e1368*, *m596*, and *sa193*. *e1365* and *sa193* have identical sequence changes (Figure 2, Table 4).

Four alleles have mutations in the CR region: *m41*, *mg43*, *m579*, and *sa187*. *m41* is a distinctive allele in that it is suppressed by *daf-12* yet relatively severe in terms of Daf-c, and Daf-c shows some maternal rescue (Gems *et al.* 1998). This allele has a G383E substitution (Yu and Larsen 2001) (reconfirmed by us). G383 is unusual in that it is conserved in all four nematode DAF-2 proteins examined, but absent from most other lineages. *m41* is the only mutation in the CR region that is not in the ligand-binding cleft (Figure 2B).

Mutations in the FnIII domains: Five *daf-2* alleles are located in the FnIII region: *e1371*, *m212*, *m577*, *mu150*, and *sa229*. *m577* has a Cys-to-Tyr mutation that disrupts an intradomain disulfide bond in the β-subunit region of the FnIII2 domain and likely destabilizes the polypeptide fold. The equivalent positions have been experimentally substituted to Ser in both *h*InsR and *h*IGF-1R, and this disulfide bond was found to be essential for correct processing and transport to the plasma membrane when the mutant receptor was expressed in COS1 cells (Maggi and Cordera 2001). *mu150* has a Gly-to-Asp substitution in the third β-strand of the FnIII1 domain. Although this Gly is not fully conserved, it is usually a small residue (Gly or Ser) in other insulin/IGF-1 receptors; possibly the bulkier side chain of Asp or its negative charge are not well tolerated in the context of neighboring structural elements.

The *m212* allele affects the α-subunit part of the insert within FnIII2. *m212* is a distinctive allele in that it has a strong temperature-sensitive Daf-c phenotype, yet is suppressed by *daf-12(m20)*. *m212* changes Cys 883 to Tyr. C883 is one of the three Cys residues (C882, C883, and C886 in DAF-2) that in *h*InsR form intermolecular disulfide bonds with the opposing α-chain (Cheatham and Kahn 1992; Schaffer and Ljungqvist 1992; Lu and Guidotti 1996; Sparrow *et al.* 1997; Wu and Guidotti 2002). The loss of this disulfide bridge may affect the quaternary structure of the receptor, perhaps accounting for the unusual properties of this allele.

Mutations in the tyrosine kinase domain: There are five *daf-2* alleles with missense mutations in the kinase domain: *sa219*, *sa223*, *e1391*, *e1370*, and *m633* (Figure 1B). *sa223*, an unusual nonconditional allele (see discussion), changes the fully conserved Arg 1430 to Gln. The equivalent residue in *h*InsR is part of the loop that determines kinase substrate selectivity (Hubbard *et al.* 1994). In *e1370*, the fully conserved Pro 1465 is replaced with a Ser. The backbone carbonyl oxygen of Pro 1465 is expected to form a hydrogen bond with the side chain of the Arg that is mutated in *sa223* and this mutation is therefore also predicted to have an effect on substrate binding. *e1391*, a severe class 2 allele, has a mutation only four residues away from *sa223* (Kimura *et al.* 1997).

DISCUSSION

We have conducted a detailed analysis and survey of 24 *daf-2* mutations. This includes phenotypic characterization of nonconditional *daf-2* alleles (including epistasis analysis), a study of allele differences in downstream effectors, sequencing of 11 new *daf-2* alleles, and modeling of the DAF-2 receptor and the likely mutational effects on its structure.

***m65* is a probable *daf-2* null mutation:** Three nonconditional alleles of *daf-2* contain nonsense mutations: *m65* (UAG, amber), *m631* (UGA, opal), and *m646* (UAA, ochre). While *m631* and *m646* are hypomorphic, *m65* is a potential null allele, despite being the most 3′ nonsense mutation. This may reflect the fact that *m65* affects a critical Trp residue in the active site of the receptor tyrosine kinase such that, if translational readthrough did occur (see below), the resulting receptor would have no tyrosine kinase activity.

Another possibility is that the truncated DAF-2 protein resulting from *m65* has a poisonous effect, such that this allele is antimorphic. However, if this were the case, one might expect *m65* to behave in a dominant-negative fashion in effects either on dauer formation (Gems *et al.* 1998) or on life span (this study), and it does not do so. The absence of any dominant effects on life span is more significant, since life span is more sensitive to the effects of reduced insulin/IGF-1 signaling than dauer formation. That *m65* is nullimorphic rather than antimorphic was also implied by an early test using the deficiency *mDf11*, which removes the *daf-2* gene region. There, *daf-2(e1370)/mDf11* and *daf-2(e1370)/daf-2(m65)* animals were shown to exhibit a similar level of dauer formation (Gems *et al.* 1998). However, the only way to be certain of the character of the *daf-2(0)* phenotype will be to delete this gene in its entirety.

A further, slight possibility is that in the *m65* strain there is a second-site mutation in a gene closely linked to *daf-2*, which enhances early larval lethality in the *daf-16; daf-2* mutant. We explored this possibility by attempting to rescue the effects of *m65* using a *pdpy-30::daf-2* transgene, which has previously been shown to rescue *daf-2(e1370)* (Wolkow *et al.* 2000). However, the transgene did not rescue the *m65* Daf-c phenotype, probably reflecting non-native *daf-2* expression from this transgene (data not shown).

The *daf-2(tm1236)* in-frame deletion removes the kinase domain and is a less severe allele than *m65*. This implies that, despite the absence of the kinase domain, some residual receptor function exists in *tm1236* mutants. One possibility is that the DAF-2 C-terminal extension, present in *tm1236* but not in *m65*, binds to and activates downstream effectors at a low level even in the absence of DAF-2 kinase activity.

Incomplete suppression of severe *daf-2* alleles by *daf-18* and *daf-16*: Using severe *daf-2* alleles, including the likely null allele *m65*, we tested whether *daf-2* mutant phenotypes are fully dependent on *daf-16* and *daf-18*, the first time that epistatic interactions between these genes have been tested using all null alleles. The increased longevity of *daf-2* mutants was fully dependent on *daf-16* but not on *daf-18*. The latter observation could mean that in the absence of DAF-2, PIP_3 is produced at a very low level, such that removal of its sink, PTEN, can only weakly restore PIP_3 levels. Alternatively, it could reflect a PIP_3-independent mechanism of life extension by *daf-2*.

The embryonic arrest and the various morphological and behavioral abnormalities in *daf-2; daf-18* and *daf-16; daf-2* mutants imply action of insulin/IGF-1 signaling in early development that warrants further investigation. These defects could reflect an early requirement for DAF-2 that is detectable only in *daf-18* or *daf-16* mutant backgrounds. By this view, severe loss of *daf-2* results in Emb and Daf-c, and only the latter may be suppressed by *daf-18* and *daf-16*. Moreover, *daf-2; daf-18* animals show some degree of dauer larva differentiation at 15°, suggesting that the *daf-18* suppressor mutation is slightly temperature sensitive.

Possible readthrough in opal and ochre but not amber nonsense mutations: Nonsense mutations are predicted to cause premature truncation of protein, which often results in a complete loss of gene function. However, some hypomorphic nonsense mutants have been reported. This can occur because the mutation is near the 3′-end of the gene, such that the truncated protein retains some activity. However, in some instances, nonsense mutations near the 5′-end of the gene are hypomorphic. This may reflect the occurrence of some translational readthrough of the nonsense codon, producing small amounts of full-length protein. This happens in opal (UGA) mutants since *C. elegans*, like many animals, has $tRNA^{[Ser]Sec}$, which can insert selenocysteine at UGA codons (Lee *et al.* 1990). Moreover, in *Escherichia coli*, third-position wobble in codon–anticodon recognition results in substitution of Trp at opal stop codons; perhaps this happens in *C. elegans*, too.

Such readthrough does not seem to happen in amber (UAG) mutants. For example, here *daf-2(m631)* (opal) is hypomorphic and *daf-2(m65)* (amber) is potentially null. Likewise, *daf-1(m40)* (opal) is hypomorphic, while four *daf-1* amber mutants all appear to be nulls (Gunther *et al.* 2000). Similarly, *lin-1(e1275)* is a hypomorphic opal (Beitel *et al.* 1995), and the hypomorphic *lon-1(sp3)* opal produces a full-length protein product (Morita *et al.* 2002). By contrast, hypomorphic amber alleles are usually found near the 3′-end of genes, *e.g.*, in *lin-1 (e1777)* (Beitel *et al.* 1995; Tuck and Greenwald 1995). Taken together, these findings suggest that, in *C. elegans*, translational readthrough occurs in opal but not in amber mutants. That the ochre mutation *daf-2(m646)* is also weaker than *daf-2(m65)* suggests that readthrough of ochre alleles may also occur, although we know of no mechanism by which this might happen.

Molecular basis of differences among nonconditional *daf-2* mutants: *daf-2* mutations may be broadly grouped into class 1 (suppressed by *daf-12*, often weaker) and class 2 (not suppressed by *daf-12*, often stronger and more pleiotropic) (Gems *et al.* 1998). Comparison of the effects of mutations in the *daf-2* gene on protein structure and phenotype allow some broad conclusions to be drawn about the molecular basis of these allele differences and suggest several new hypotheses.

First, apart from *e1369* (which seems to lie beyond the *daf-2* open reading frame), all class 1 mutations map to the CR, L2, and FnIII domains of the extracellular part of the receptor. Structural modeling implies that these mutations do not directly affect ligand contact residues, but instead cause subtle changes in the conformation of the extracellular domain. Studies in mammalian cells have shown that this can lead to mis-processing of the proreceptor and to a reduced number of functional receptors at the cell surface. Interestingly, mutations affecting the same residues as the class 1 alleles *m577* and *m596* have been studied in the human insulin receptor and have this effect (see RILM at http://www.biochem.ucl.ac.uk/rilm/) (Garza-Garcia *et al.* 2007). Possibly, reduced DAF-2 protein levels typify class 1 *daf-2* mutants.

Second, class 2 and nonconditional alleles either map to the tyrosine kinase domain or cluster around the predicted ligand-binding cleft formed by parts of the L1 and CR domains (Figure 2B). It has been suggested that the properties of class 1 alleles (*e.g.*, *e1368*) might reflect effects on ligand binding (Hsin and Kenyon 1999). However, the distribution of lesions in DAF-2 (Figure 2B) argues against this interpretation. Third, none of the 24 mutations lie in the N-terminal and C-terminal extension regions of DAF-2, hinting (although certainly not proving) that these play a relatively minor role in DAF-2 function. Fourth, each of the atypical class 1 alleles (*i.e.*, those that are more severe in terms of Daf-c than many class 2 alleles) is idiosyncratic in terms of its molecular lesion. For example, the *m41* lesion lies in a structurally obscure region of DAF-2 present only in nematodes; *m212* may affect function at the level of quaternary structure; and the most atypical class 1 allele, *e1369*, appears to lie outside of the *daf-2* open reading frame.

The results described here provide a more nuanced description of *daf-2* allelic variation than the previously defined class 1/class 2 allele distinction, as follows. First, overall severity defines a basic allelic series, to which many alleles conform. For example, differences in effects of *m577* (class 1) and *e1370* (class 2) on signaling effectors reveal only that *e1370* is more a severe allele. Second, the class 1/class 2 distinction is necessary, given

the unusual alleles that are severely Daf-c yet not suppressed by *daf-12*: atypical class 1 alleles such as *e1369*, *m41*, and *m212*.

Potential complex effects on signaling in some class 2 *daf-2* alleles: Our analysis also suggests a new hypothesis relating to class 2 *daf-2* mutants. Signaling into the cell from insulin/IGF-1 receptors involves several pathways (Nanji *et al.* 2005). Potentially, some aspects of *daf-2* allele differences reflect differential effects of mutation on signaling via the PIP_3 and other pathways, *e.g.*, *let-60*/Ras (Nanji *et al.* 2005). For example, *daf-2(sa223)* is an unusual allele, which results in nonconditional predauer (L2d) arrest that can be maternally rescued (Malone and Thomas 1994; Gems *et al.* 1998). *daf-2(sa223)* homozygotes derived from *daf-2(sa223)*/+ mothers form dauer larvae at 25°, but few or none at lower temperatures. *sa223* results in R1430Q, and the equivalent mutation, R1174Q, has been found in *h*InsR in several patients with type A insulin resistance (Moller *et al.* 1994; Moritz *et al.* 1994) (in each case, the individual was heterozygous for the mutation). The effects of this mutation in the homozygous state were characterized by expression in CHO cells and found to cause impairment of insulin-stimulated receptor tyrosine phosphorylation, glycogen synthesis, and mitogenesis (Krook *et al.* 1996). Interestingly, however, insulin-stimulated IRS-1 phosphorylation and recruitment of PI 3-kinase was not fully blocked and at high concentrations of insulin it approached wild-type levels (Krook *et al.* 1996, 1997). However, there was an absence of insulin-stimulated tyrosine phosphorylation of *S*rc *h*omologous and *c*ollagen-like (Shc), GTP loading of Ras, and MAP kinase activation. Shc is an adaptor protein that binds to various activated receptors, usually at the PTB domain. *daf-2(e1391)* is equivalent to the human IR mutation P1178L (Kim *et al.* 1992; Krook *et al.* 1994; Kimura *et al.* 1997), which has effects on receptor function similar to the *sa223*-equivalent R1174Q (Krook *et al.* 1996, 1997).

A third allele, *daf-2(m579)*, results in R437C, equivalent to *h*InsR R252C, which is found in the homozygous state in subjects with type A insulin resistance (Hamer *et al.* 2002). It is therefore a less severe defect than the human equivalents of *sa223* and *e1391*, which cause severe insulin resistance in the heterozygous state (Kim *et al.* 1992; Krook *et al.* 1994; Moller *et al.* 1994). However, it too results in severe reduction of signaling through Shc, but has little effect on activation of PI 3-kinase (Hamer *et al.* 2002). In this case, the authors suggest that the PI 3-kinase pathway activation may be due to demonstrably reduced endocytosis of the ligand-bound receptor, resulting in increased perdurance of the activated receptor signal. Enhancement of receptor signaling has also been observed in the EGF receptor upon inhibition of clathrin-mediated endocytosis (Vieira *et al.* 1996). Consistent with this, mutation of *unc-101*, which encodes a homolog of the AP47 clathrin-associated protein, suppresses hypomorphic alleles of the *let-23* EGF receptor gene (Lee *et al.* 1994). Such a combination of overall reduction of insulin/IGF-1 receptor function, combined with selective rescue of PI 3-kinase signaling, may be a common characteristic among class 2 *daf-2* mutants.

Conclusions: Our study suggests the following overview of *daf-2* allele variation: *daf-2* mutations form a very approximate allelic series in which weaker alleles are often class 1, and more severe alleles are often class 2. A number of class 1 alleles are atypical and do not conform to this series, being unusually severe in terms of Daf-c. Mutations in class 1 alleles occur only in some regions of the receptor ectodomain while class 2 alleles are clustered in the ligand-binding cleft and the kinase domain. The mutations in atypical class 1 alleles each have idiosyncratic effects, whose outcome remains to be established. In class 2 alleles, signaling pathways other than PIP_3-dependent signaling may be disproportionately impaired, as suggested by the properties of similar mutations in humans. The most severe loss of function in *daf-2* results in recessive early embryonic lethality and effects on life span that are fully dependent on *daf-16* but not on *daf-18*.

We thank Sindhuja Kadambi and Diana McCulloch for help with sequencing; Adam Antebi and Naoto Ueno for useful discussion; Cynthia Kenyon, Don Riddle, and Jim Thomas for providing *daf-2* alleles; Kotaro Kimura and Gary Ruvkun for sharing information; and Ken Kemphues for a helpful critique of the manuscript. Some strains were provided by the *Caenorhabditis* Genetics Center, which is funded by the National Institutes of Health National Center for Research Resources. This work was supported by the Biotechnology and Biological Sciences Research Council (UK), the European Union (Framework V), and the Wellcome Trust.

LITERATURE CITED

Antebi, A., W. Yeh, D. Tait, E. Hedgecock and D. Riddle, 2000 *daf-12* encodes a nuclear receptor that regulates the dauer diapause and developmental age in *C. elegans*. Genes Dev. **14:** 1512–1527.

Avery, L., and S. Wasserman, 1992 Ordering gene function: the interpretation of epistasis in regulatory hierarchies. Trends Genet. **8:** 312–316.

Ayyadevara, S., R. Alla, J. J. Thaden and R. J. Shmookler Reis, 2007 Remarkable longevity and stress resistance of nematode PI3K-null mutants. Aging Cell **7:** 13–22.

Beitel, G., S. Tuck, I. Greenwald and H. Horvitz, 1995 The *Caenorhabditis elegans* gene *lin-1* encodes an ETS-domain protein and defines a branch of the vulval induction pathway. Genes Dev. **9:** 3149–3162.

Bluher, M., B. Kahn and C. Kahn, 2003 Extended longevity in mice lacking the insulin receptor in adipose tissue. Science **299:** 572–574.

Brenner, S., 1974 The genetics of *Caenorhabditis elegans*. Genetics **77:** 71–94.

Cassada, R. C., and R. L. Russell, 1975 The dauerlarva, a post-embryonic developmental variant of the nematode *Caenorhabditis elegans*. Dev. Biol. **46:** 326–342.

Cheatham, B., and C. R. Kahn, 1992 Cysteine 647 in the insulin receptor is required for normal covalent interaction between alpha- and beta-subunits and signal transduction. J. Biol. Chem. **267:** 7108–7115.

Choe, S. E., M. Boutros, A. M. Michelson, G. M. Church and M. S. Halfon, 2005 Preferred analysis methods for Affymetrix GeneChips revealed by a wholly defined control dataset. Genome Biol. **6:** R16.

Clancy, D., D. Gems, L. G. Harshman, S. Oldham, E. Hafen *et al.*, 2001 Extension of lifespan by loss of *chico*, a *Drosophila* insulin receptor substrate protein. Science **292:** 104–106.

Friedman, D. B., and T. E. Johnson, 1988 A mutation in the *age-1* gene in *Caenorhabditis elegans* lengthens life and reduces hermaphrodite fertility. Genetics **118:** 75–86.

Gandhi, S., J. Santelli, D. G. Mitchell, J. W. Stiles and D. Raosanadi, 1980 A simple method for maintaining large, aging populations of *Caenorhabditis elegans*. Mech. Ageing Dev. **12:** 137–150.

Garigan, D., A. Hsu, A. Fraser, R. Kamath, J. Ahringer *et al.*, 2002 Genetic analysis of tissue aging in *Caenorhabditis elegans*: a role for heat-shock factor and bacterial proliferation. Genetics **161:** 1101–1112.

Garza-Garcia, A., D. S. Patel, D. Gems and P. C. Driscoll, 2007 RILM: a web-based resource to aid comparative and functional analysis of the insulin and IGF-1 receptor family. Hum. Mutat. **28:** 660–668.

Gems, D., and D. L. Riddle, 2000 Defining wild-type life span in *Caenorhabditis elegans*. J. Gerontol. A Biol. Sci. Med. Sci. **55:** B215–B219.

Gems, D., A. J. Sutton, M. L. Sundermeyer, P. L. Larson, P. S. Albert *et al.*, 1998 Two pleiotropic classes of *daf-2* mutation affect larval arrest, adult behavior, reproduction and longevity in *Caenorhabditis elegans*. Genetics **150:** 129–155.

Gerisch, B., C. Weitzel, C. Kober-Eisermann, V. Rottiers and A. Antebi, 2001 A hormonal signaling pathway influencing *C. elegans* metabolism, reproductive development, and life span. Dev. Cell **1:** 841–851.

Gil, E., E. Malone Link, L. Liu, C. Johnson and J. Lees, 1999 Regulation of the insulin-like developmental pathway of *Caenorhabditis elegans* by a homolog of the PTEN tumor suppressor gene. Proc. Natl. Acad. Sci. USA **96:** 2925–2930.

Gottlieb, S., and G. Ruvkun, 1994 *daf-2, daf-16* and *daf-23*: genetically interacting genes controlling dauer formation in *Caenorhabditis elegans*. Genetics **137:** 107–120.

Gunther, C., L. Georgi and D. Riddle, 2000 A *Caenorhabditis elegans* type I TGF beta receptor can function in the absence of type II kinase to promote larval development. Development **127:** 3337–3347.

Hamer, I., M. Foti, R. Emkey, M. Cordier-Bussat, J. Philippe *et al.*, 2002 An arginine to cysteine(252) mutation in insulin receptors from a patient with severe insulin resistance inhibits receptor internalisation but preserves signalling events. Diabetologia **45:** 657–667.

Henderson, S. T., and T. E. Johnson, 2001 *daf-16* integrates developmental and environmental inputs to mediate aging in the nematode *Caenorhabditis elegans*. Curr. Biol. **11:** 1975–1980.

Hertweck, M., C. Gobel and R. Baumeister, 2004 *C. elegans* SGK-1 is the critical component in the Akt/PKB kinase complex to control stress response and life span. Dev. Cell **6:** 577–588.

Holzenberger, M., J. Dupont, B. Ducos, P. Leneuve, A. Geloen *et al.*, 2003 IGF-1 receptor regulates lifespan and resistance to oxidative stress in mice. Nature **421:** 182–187.

Hopper, N. A., 2006 The adaptor protein soc-1/Gab1 modifies growth factor receptor output in *Caenorhabditis elegans*. Genetics **173:** 163–175.

Hsin, H., and C. Kenyon, 1999 Signals from the reproductive system regulate the lifespan of *C. elegans*. Nature **399:** 362–366.

Hsu, A., C. Murphy and C. Kenyon, 2003 Regulation of aging and age-related disease by DAF-16 and heat-shock factor. Science **300:** 1142–1145.

Huang, L. S., and P. W. Sternberg, 1995 Genetic dissection of developmental pathways, pp. 98–122 in *Caenorhabditis elegans: Modern Biological Analysis of an Organism*, edited by H. F. Epstein and D. C. Shakes. Academic Press, San Diego.

Hubbard, S., L. Wei, L. Ellis and W. Hendrickson, 1994 Crystal structure of the tyrosine kinase domain of the human insulin receptor. Nature **372:** 746–754.

Kenyon, C., J. Chang, E. Gensch, A. Rudener and R. Tabtiang, 1993 A *C. elegans* mutant that lives twice as long as wild type. Nature **366:** 461–464.

Kim, H., H. Kadowaki, H. Sakura, M. Odawara, K. Momomura *et al.*, 1992 Detection of mutations in the insulin receptor gene in patients with insulin resistance by analysis of single-stranded conformational polymorphisms. Diabetologia **35:** 261–266.

Kimura, K. D., H. A. Tissenbaum, Y. Liu and G. Ruvkun, 1997 *daf-2*, an insulin receptor-like gene that regulates longevity and diapause in *Caenorhabditis elegans*. Science **277:** 942–946.

Krook, A., S. Kumar, I. Laing, A. J. Boulton, J. A. Wass *et al.*, 1994 Molecular scanning of the insulin receptor gene in syndromes of insulin resistance. Diabetes **43:** 357–368.

Krook, A., D. E. Moller, K. Dib and S. O'Rahilly, 1996 Two naturally occurring mutant insulin receptors phosphorylate insulin receptor substrate-1 (IRS-1) but fail to mediate the biological effects of insulin. Evidence that IRS-1 phosphorylation is not sufficient for normal insulin action. J. Biol. Chem. **271:** 7134–7140.

Krook, A., J. P. Whitehead, S. P. Dobson, M. R. Griffiths, M. Ouwens *et al.*, 1997 Two naturally occurring insulin receptor tyrosine kinase domain mutants provide evidence that phosphoinositide 3-kinase activation alone is not sufficient for the mediation of insulin's metabolic and mitogenic effects. J. Biol. Chem. **272:** 30208–30214.

Labbe, J., J. Burgess, L. Rokeach and S. Hekimi, 2000 ROP-1, an RNA quality-control pathway component, affects *Caenorhabditis elegans* dauer formation. Proc. Natl. Acad. Sci. USA **97:** 13233–13238.

Larsen, P. L., P. S. Albert and D. L. Riddle, 1995 Genes that regulate both development and longevity in *Caenorhabditis elegans*. Genetics **139:** 1567–1583.

Lee, B., M. Rajagopalan, Y. Kim, K. You, K. Jacobson *et al.*, 1990 Selenocysteine tRNA[Ser]Sec gene is ubiquitous within the animal kingdom. Mol. Cell. Biol. **10:** 1940–1949.

Lee, J., G. Jongeward and P. Sternberg, 1994 *unc-101*, a gene required for many aspects of *Caenorhabditis elegans* development and behavior, encodes a clathrin-associated protein. Genes Dev. **8:** 60–73.

Lee, R., J. Hench and G. Ruvkun, 2001 Regulation of *C. elegans* DAF-16 and its human orthologue FKHRL1 by the *daf-2* insulin-like signaling pathway. Curr. Biol. **11:** 1950–1957.

Lin, K., J. B. Dorman, A. Rodan and C. Kenyon, 1997 *daf-16*: an HNF-3/forkhead family member that can function to double the life-span of *Caenorhabditis elegans*. Science **278:** 1319–1322.

Lin, K., H. Hsin, N. Libina and C. Kenyon, 2001 Regulation of the *Caenorhabditis elegans* longevity protein DAF-16 by insulin/IGF-1 and germline signaling. Nat. Genet. **28:** 139–145.

Lu, K., and G. Guidotti, 1996 Identification of the cysteine residues involved in the class I disulfide bonds of the human insulin receptor: properties of insulin receptor monomers. Mol. Biol. Cell **7:** 679–691.

Ludewig, A., C. Kober-Eisermann, C. Weitzel, A. Bethke, K. Neubert *et al.*, 2004 A novel nuclear receptor/coregulator complex controls *C. elegans* lipid metabolism, larval development, and aging. Genes Dev. **18:** 2120–2133.

Maggi, D., and R. Cordera, 2001 Cys 786 and Cys 776 in the post-translational processing of the insulin and IGF-I receptors. Biochem. Biophys. Res. Commun. **280:** 836–841.

Malone, E. A., and J. H. Thomas, 1994 A screen for nonconditional dauer-constitutive mutations in *Caenorhabditis elegans*. Genetics **136:** 879–886.

McElwee, J. J., E. Schuster, E. Blanc, J. H. Thomas and D. Gems, 2004 Shared transcriptional signature in *C. elegans* dauer larvae and long-lived *daf-2* mutants implicates detoxification system in longevity assurance. J. Biol. Chem. **279:** 44533–44543.

Mihaylova, V., C. Borland, L. Manjarrez, M. Stern and H. Sun, 1999 The PTEN tumor suppressor homolog in *Caenorhabditis elegans* regulates longevity and dauer formation in an insulin receptor-like signaling pathway. Proc. Natl. Acad. Sci. USA **96:** 7427–7432.

Moller, D. E., O. Cohen, Y. Yamaguchi, R. Assiz, F. Grigorescu *et al.*, 1994 Prevalence of mutations in the insulin receptor gene in subjects with features of the type A syndrome of insulin resistance. Diabetes **43:** 247–255.

Morita, K., A. J. Flemming, Y. Sugihara, M. Mochii, Y. Suzuki *et al.*, 2002 A *Caenorhabditis elegans* TGF-beta, DBL-1, controls the expression of LON-1, a PR-related protein, that regulates polyploidization and body length. EMBO J. **21:** 1063–1073.

Moritz, W., E. Froesch and M. Boni-Schnetzler, 1994 Functional properties of a heterozygous mutation (Arg1174→Gln) in the tyrosine kinase domain of the insulin receptor from a type A insulin resistant patient. FEBS Lett. **351:** 276–280.

Morris, J. Z., H. A. Tissenbaum and G. Ruvkun, 1996 A phosphatidylinositol-3-OH kinase family member regulating longevity and diapause in *Caenorhabditis elegans*. Nature **382:** 536–538.

Motola, D. L., C. L. Cummins, V. Rottiers, K. K. Sharma, T. Li *et al.*, 2006 Identification of ligands for DAF-12 that govern dauer formation and reproduction in *C. elegans*. Cell **124:** 1209–1223.

Murphy, C. T., S. A. McCarroll, C. I. Bargmann, A. Fraser, R. S. Kamath *et al.*, 2003 Genes that act downstream of DAF-16 to influence the lifespan of *C. elegans*. Nature **424:** 277–284.

Nanji, M., N. A. Hopper and D. Gems, 2005 LET-60 RAS modulates effects of insulin/IGF-1 signaling on development and aging in Caenorhabditis elegans. Aging Cell **4:** 235–245.

Ogg, S., and G. Ruvkun, 1998 The *C. elegans* PTEN homolog, DAF-18, acts in the insulin receptor-like metabolic signaling pathway. Mol. Cell **2:** 887–893.

Ogg, S., S. Paradis, S. Gottlieb, G. I. Patterson, L. Lee *et al.*, 1997 The Fork head transcription factor DAF-16 transduces insulin-like metabolic and longevity signals in *C. elegans*. Nature **389:** 994–999.

Paradis, S., and G. Ruvkun, 1998 *Caenorhabditis elegans* Akt/PKB transduces insulin receptor-like signals from AGE-1 PI3 kinase to the DAF-16 transcription factor. Genes Dev. **12:** 2488–2498.

Paradis, S., M. Ailion, A. Toker, J. H. Thomas and G. Ruvkun, 1999 A PDK1 homolog is necessary and sufficient to transduce AGE-1 PI3 kinase signals that regulate diapause in *Caenorhabditis elegans*. Genes Dev. **13:** 1438–1452.

Pierce, S. B., M. Costa, R. Wisotzkey, S. Devadhar, S. A. Homburger *et al.*, 2001 Regulation of DAF-2 receptor signaling by human insulin and *ins-1*, a member of the unusually large and diverse *C. elegans* insulin gene family. Genes Dev. **15:** 672–686.

Riddle, D. L., and P. S. Albert, 1997 Genetic and environmental regulation of dauer larva development, pp. 739–768 in *C. elegans II*, edited by D. L. Riddle, T. Blumenthal, B. J. Meyer and J. R. Priess. Cold Spring Harbor Laboratory Press, Plainview, NY.

Rouault, J., P. E. Kuwabara, O. M. Sinilnikova, L. Duret, D. Thierry-Mieg *et al.*, 1999 Regulation of dauer larva development in *Caenorhabditis elegans* by *daf-18*, a homologue of the tumour suppressor PTEN. Curr. Biol. **9:** 329–332.

Schaffer, L., and L. Ljungqvist, 1992 Identification of a disulfide bridge connecting the alpha-subunits of the extracellular domain of the insulin receptor. Biochem. Biophys. Res. Commun. **189:** 650–653.

Schuster, E. F., E. Blanc, L. Partridge and J. M. Thornton, 2007 Estimation and correction of non-specific binding in a large-scale spike-in experiment. Genome Biol. **8:** R126.

Scott, B., M. Avidan and C. Crowder, 2002 Regulation of hypoxic death in *C. elegans* by the insulin/IGF receptor homolog DAF-2. Science **296:** 2388–2391.

Shim, J., S. Im and J. Lee, 2003 Tissue-specific expression, heat inducibility, and biological roles of two *hsp16* genes in *Caenorhabditis elegans*. FEBS Lett. **537:** 139–145.

Sparrow, L. G., N. M. McKern, J. J. Gorman, P. M. Strike, C. P. Robinson *et al.*, 1997 The disulfide bonds in the C-terminal domains of the human insulin receptor ectodomain. J. Biol. Chem. **272:** 29460–29467.

Sulston, J., and J. Hodgkin, 1988 Methods, pp. 587–606 in *The Nematode Caenorhabditis elegans*, edited by W. B. Wood. Cold Spring Harbor Laboratory Press, Plainview, NY.

Tatar, M., A. Kopelman, D. Epstein, M.-P. Tu, C.-M. Yin *et al.*, 2001 Mutations in the Drosophila insulin receptor homologue retard senescence and impair neuroendocrine function. Science **292:** 107–110.

Taylor, S., A. Cama, D. Accili, F. Barbetti, M. Quon *et al.*, 1992 Mutations in the insulin receptor gene. Endocr. Rev. **13:** 566–595.

Tuck, S., and I. Greenwald, 1995 *lin-25*, a gene required for vulval induction in *Caenorhabditis elegans*. Genes Dev. **9:** 341–357.

Vieira, A., C. Lamaze and S. Schmid, 1996 Control of EGF receptor signaling by clathrin-mediated endocytosis. Science **274:** 2086–2089.

Vowels, J. J., and J. H. Thomas, 1992 Genetic analysis of chemosensory control of dauer formation in *Caenorhabditis elegans*. Genetics **130:** 105–123.

Walker, G. A., and G. J. Lithgow, 2003 Lifespan extension in *C. elegans* by a molecular chaperone dependent upon insulin-like signals. Aging Cell **2:** 131–139.

Walker, G., T. White, G. McColl, N. Jenkins, S. Babich *et al.*, 2001 Heat shock protein accumulation is upregulated in a long-lived mutant of *Caenorhabditis elegans*. J. Gerontol. A Biol. Sci. Med. Sci. **56:** B281–B287.

Whittaker, J., and L. Whittaker, 2005 Characterization of the functional insulin binding epitopes of the full-length insulin receptor. J. Biol. Chem. **280:** 20932–20936.

Wolkow, C., K. Kimura, M. Lee and G. Ruvkun, 2000 Regulation of *C. elegans* life-span by insulinlike signaling in the nervous system. Science **290:** 147–150.

Wolkow, C., M. Munoz, D. Riddle and G. Ruvkun, 2002 Insulin receptor substrate and p55 orthologous adaptor proteins function in the *Caenorhabditis elegans daf-2*/insulin-like signaling pathway. J. Biol. Chem. **277:** 49591–49597.

Wu, J. J., and G. Guidotti, 2002 Construction and characterization of a monomeric insulin receptor. J. Biol. Chem. **277:** 27809–27817.

Yu, H., and P. Larsen, 2001 DAF-16-dependent and independent expression targets of DAF-2 insulin receptor-like pathway in *Caenorhabditis elegans* include FKBPs. J. Mol. Biol. **314:** 1017–1028.

Communicating editor: M. Nonet